Important note: The present paper work was sent to International Journal of Solids and Structures on 23 March 2020 (it is currently under review).

The octahedron family: a source of tensegrity structures

Manuel Alejandro Fernández-Ruiz[a,*], Enrique Hernández-Montes[b], Luisa María Gil-Martín[c]

[a] Department of Industrial and Civil Engineering, University of Cádiz (UCA). Campus Bahía de Algeciras, Avda. Ramón Puyol, s/n. 11201 Algeciras (Cádiz), Spain. manuelalejandro.fernandez@uca.es. *Corresponding author

[b] Department of Structural Mechanics, University of Granada (UGR). Campus Universitario de Fuentenueva s/n. 18072 Granada, Spain. emontes@ugr.es.

[c] Department of Structural Mechanics, University of Granada (UGR). Campus Universitario de Fuentenueva s/n. 18072 Granada, Spain. mlgil@ugr.es.

Abstract

A tensegrity family is a group of tensegrity structures that share a common connectivity pattern. In the case that just two values of the force density or force:length ratio are adopted (one for cables and another for struts), the members of the octahedron family are: the octahedron, the expanded octahedron and the double-expanded octahedron. In this work a higher number of possible force:length ratio values have been considered in order to find new members of the family. The values of the force:length ratios which satisfy the super-stability conditions have been computed analytically. New super-stable tensegrity forms of the octahedron family have been obtained. Results show that all of them are members of the octahedron family having as folded forms all the lower

members of the family. Finally, based on topological rules, it has been proved that the double-expanded octahedron can be defined from a truncated cube.

1. Introduction

Tensegrity, a structure composed by pre-stressed pin-jointed compression (struts) and tension (cables) members that are self-equilibrated, was firstly introduced by Fuller (Fuller, 1975). Tensegrity structures have had a great development in the last years due to their unique mechanical and mathematical properties in comparison with conventional structural forms such as trusses and frames (Zhang and Ohsaki, 2015). In biology, the principles of tensegrity structures have been used in cells (Ingber, 2003, 1993) and tissues (Maina, 2007). In industrial and civil engineering tensegrity structures have a wide variety of applications such as deployable aerospace devices (Tibert and Pellegrino, 2002), robotic (Graells Rovira and Mirats Tur, 2009) and civil engineering works (Rhode-Barbarigos et al., 2010).

The two key aspects in the design of tensegrity structures are the self-equilibrium and the (super-)stability (Zhang and Ohsaki, 2015). The cables and struts of a tensegrity carry axial forces even when no external load is applied (self-stresses). The geometrical configuration and the prestress state of cables and struts are interdependent with each other. This is the main difficulty in finding an equilibrium shape of a tensegrity. The problem of determining the self-equilibrated configuration is called form-finding. Tibert and Pellegrino (Tibert and Pellegrino, 2003) presented a review of form-finding methods of tensegrity structures. The Force Density Method (FDM) is one of the most

used form-finding methods of pin-jointed networks (Linkwitz and Schek, 1971; Schek, 1974). The equilibrium equations (which are highly nonlinear) are linearized introducing the concept of force:length ratio or force density q. The FDM has been widely used in several form-finding methods of tensegrity structures (Tran and Lee, 2010; Vassart and Motro, 1999; Zhang and Ohsaki, 2006). The dynamic relaxation method introduced by Otter (Otter, 1965) has also been used in the form-finding problem of tensegrity structures (Bel Hadj Ali et al., 2011; Motro, 1984).

The existing form-finding methods can be classified into two categories: numerical and analytical. Numerical methods are used to solve the form-finding problem of complex tensegrity structures with a high number of members. In the literature there are many works related to numerical form-finding methods; examples of them can be seen in (Estrada et al., 2006; Masic et al., 2005; Tran and Lee, 2010; Zhang and Ohsaki, 2006). On the other hand, analytical methods are usually used for simple tensegrities with a relatively small number of members or high symmetry. There are not so many works in the literature about analytical form-finding methods of tensegrity structures (M.A. Fernández-Ruiz et al., 2019a; Hernández-Montes et al., 2018; Vassart and Motro, 1999; Zhang et al., 2013). Analytical form-finding methods achieve the equilibrium shape through a symbolic analysis. In general, some symmetric properties of the resultant tensegrity are enforced in order to simplify the form-finding problem. In fact, symmetry has been a great source of new tensegrity forms (Masic et al., 2005). Other source of tensegrity forms are the so-called "truncated regular polyhedral tensegrities", which are obtained from geometrical forms (Zhang and Ohsaki, 2012; Zhang et al., 2013, 2012). Analytical form-finding methods give a deep understanding of both the geometry and the self-stress state of the tensegrity. On the contrary, numerical methods only give a discrete solution of the self-equilibrium state.

The other key aspect in the design of tensegrity structures is the stability. The super-stability is a robust stability criterion for tensegrity structures (Connelly, 1998; Zhang and Ohsaki, 2007). A tensegrity structure is said to be super-stable if it is always stable for any level of self-stress and material properties considered (Connelly, 1998; Zhang and Ohsaki, 2007). In super-stable tensegrities, an increase of the prestress of their members tend to stiffen them (Connelly and Back, 1998), which is an important property for the potential applications of tensegrities in both industrial and civil engineering.

A tensegrity family is defined as a group of tensegrity structures that share the same connectivity pattern (Fernández-Ruiz et al., 2019a). Each tensegrity has a position into the family, in such a way that it has as folded forms all the lower members of the family. Folded forms are tensegrity structures where some nodes in the equilibrium shape share the same position in the space (Hernández-Montes et al., 2018). On the other hand, full forms are defined as tensegrity structures whose nodes in the equilibrium configuration have different coordinates (Hernández-Montes et al., 2018). The authors introduced in a previous work the octahedron family (Fernández-Ruiz et al., 2019a), which is made up of the octahedron, the expanded octahedron and the double-expanded octahedron. In the form-finding process of these three tensegrities only two possible values of q were considered (i.e., one for cables and another one for struts). The possibility of considering a higher number of possible values of q was studied in (Fernández-Ruiz et al., 2019b).

In this work the octahedron family is presented as a source of tensegrity forms. New super-stable tensegrity forms are derived from the connectivity pattern of the octahedron family considering a higher number of different force:length ratio values. Unlike other sources of tensegrity structures based on symmetry and geometrical forms,

in this work new tensegrity forms are obtained based on the connectivity pattern (topology) of the octahedron family. Finally, it is proved that the double-expanded octahedron (obtained following the connectivity pattern of the octahedron family) can be geometrically obtained from a truncated cube if an appropriate connectivity pattern is adopted.

2. Self-equilibrium, rank deficiency and super-stability of tensegrity structures

2.1 Self-equilibrium of tensegrity structures

The FDM introduced in (Schek, 1974) is a form finding method for general networks. The equilibrium of a mesh with n free nodes, n_f fixed nodes and m members is obtained considering constant values of force:length ratio to each member of the mesh. Free nodes are free to move in the space, while fixed nodes act as supports. The force:length ratio or force density q_j of the jth member is defined as the ratio between the axial force and the length of the member jth of the mesh. The connectivity matrix $\mathbf{C_S}$ ($\in \Re^{m \times (n+nf)}$) shows the connectivity between the nodes of the mesh; it can be easily defined based on topological rules as described in (Hernández-Montes et al., 2006). The connectivity matrix is constructed in the following way: if a general member j connects nodes i and k (with $i < k$), the ith and kth elements of the jth row of $\mathbf{C_S}$ are set to 1 and -1 respectively (see Eq. (1)).

$$\mathbf{C_S}(j,r) = \begin{cases} +1 & \text{if } i(j) = r \\ -1 & \text{if } k(j) = r \\ 0 & \text{otherwise} \end{cases} \tag{1}$$

As it is proposed by Schek (Schek, 1974), $\mathbf{C_S}$ can be partitioned into two matrices $\mathbf{C}$ ($\in \Re^{m \times n}$) and $\mathbf{C_f}$ ($\in \Re^{m \times nf}$) if the fixed nodes are numbered first ($\mathbf{C_S} = [\mathbf{C}\ \mathbf{C_f}]$). Let us denote $\mathbf{x}$, $\mathbf{y}$, $\mathbf{z}$ ($\in \Re^n$) and $\mathbf{x_f}$, $\mathbf{y_f}$, $\mathbf{z_f}$ ($\in \Re^{nf}$) as the nodal coordinate vectors in x, y and z directions of free and fixed nodes respectively. The external forces applied at the free

5

nodes in the x, y and z directions are collected in the vectors $\mathbf{P_x}$, $\mathbf{P_y}$ and $\mathbf{P_z}$ ($\in \Re^n$) respectively. Then, the equilibrium equations of a general pin-jointed network are shown in Eq. (2) as proposed in (Schek, 1974).

$$\begin{aligned}
\mathbf{C}^T\mathbf{Q}\mathbf{C}\mathbf{x} + \mathbf{C}^T\mathbf{Q}\mathbf{C_f}\mathbf{x_f} &= \mathbf{P_x} \\
\mathbf{C}^T\mathbf{Q}\mathbf{C}\mathbf{y} + \mathbf{C}^T\mathbf{Q}\mathbf{C_f}\mathbf{y_f} &= \mathbf{P_y} \\
\mathbf{C}^T\mathbf{Q}\mathbf{C}\mathbf{z} + \mathbf{C}^T\mathbf{Q}\mathbf{C_f}\mathbf{z_f} &= \mathbf{P_z}
\end{aligned} \tag{2}$$

In Eq. (2) $\mathbf{Q}$ ($\in \Re^{m \times m}$) is the diagonal square matrix of the vector $\mathbf{q}$ ($\in \Re^m$) that contains the force:length ratio of each branch. The symbol $[]^T$ represents the transpose operation of a matrix or vector.

In tensegrity structures external forces are ignored (self-stressed equilibrium) and fixed nodes are not required because they are free-standing structures ($n_f = 0$). In this context, the equilibrium equations of a general tensegrity can be formulated as:

$$\begin{aligned}
\mathbf{D}\mathbf{x} &= 0 \\
\mathbf{D}\mathbf{y} &= 0 \\
\mathbf{D}\mathbf{z} &= 0
\end{aligned} \tag{3}$$

where $\mathbf{D} = \mathbf{C}^T\mathbf{Q}\mathbf{C}$ ($\in \Re^{n \times n}$) is the force density matrix.

2.2 Rank deficiency

In the case of tension (Hernández-Montes et al., 2006) and compression (Fernández-Ruiz et al., 2017) structures where the force:length ratio values of all the members of the mesh are of the same sign ($q > 0$ in tension and $q < 0$ in compression) and fixed nodes are present, the form-finding problem is well-solved (Levy and Spillers, 2004) because its corresponding matrix $\mathbf{D}$ is nonsingular. Therefore, $\mathbf{D}$ can be inverted and the positions of the free nodes are computed solving Eq. (2). In the case of compression structures with prestressing tendons, some additional conditions must be fulfilled in the determination of an equilibrium configuration (Fernández-Ruiz et al., 2019c).

In the case of tensegrity structures, tension (cables) and compression (struts) members coexist. By construction of **D**, the sum of the elements of each row or a column is zero. Consequently, **D** is always singular and the equilibrium configuration is not obtained directly from Eq. (2) as in both compression and tension structures. It can be proved that a tensegrity of dimension d has a force density matrix with a rank deficiency of at least $d+1$ (Hernández-Montes et al., 2018; Zhang and Ohsaki, 2006) (non-degeneracy condition). This condition is achieved imposing that the characteristic polynomial (see Eq. (4)) corresponding to the force density matrix has $d + 1$ zero roots. Consequently, coefficients a_3, a_2, a_1 and a_0 of the characteristic polynomial must be zero in order to obtain a three-dimensional (3D) tensegrity. As matrix **D** is always singular, coefficient a_0 is always 0. So, if the three coefficients a_3, a_2 and a_1 are set to zero a system of polynomial equations in terms of the force:length ratios of the members of the 3D tensegrity is provided. This system of equations can be solved analytically if some relations between the force:length ratio of the members are imposed (Fernández-Ruiz et al., 2019a; Hernández-Montes et al., 2018; Zhang et al., 2013) (see Eq. (5)).

$$p(\lambda)=\lambda^n+a_{n-1}\lambda^{n-1}+\ldots+a_1\lambda+a_0 \tag{4}$$

$$
\begin{aligned}
a_3(q_1,\ldots,q_m) &= 0 \\
a_2(q_1,\ldots,q_m) &= 0 \\
a_1(q_1,\ldots,q_m) &= 0
\end{aligned}
\tag{5}
$$

A more detailed description of the analytical form-finding procedure used in this work can be seen in (Fernández-Ruiz et al., 2019a; Hernández-Montes et al., 2018).

2.3 Super-stability of tensegrity structures

A tensegrity which is always stable, regardless of material properties and prestress, is called super-stable (Connelly, 1998; Zhang and Ohsaki, 2007). The super-stability conditions of tensegrities are the following (Connelly, 1998; Zhang and Ohsaki, 2015, 2007):

i.   The rank deficiency of the force density matrix **D** is exactly $d + 1$.

ii.   The force density matrix **D** is positive semi-definite.

iii. The rank of the matrix **G**, defined in Eq. (6) is $(d^2 + d)/2$.

$$\mathbf{G} = \left(\mathbf{Uu}, \mathbf{Vv}, \mathbf{Ww}, \mathbf{Uv}, \mathbf{Uw}, \mathbf{Vw} \right) \tag{6}$$

Matrix **G** is called the geometry matrix because it is only related to the geometry of the structure. A deeper explanation about matrix **G** can be seen in (Zhang and Ohsaki, 2015). The stability of tensegrity structures has been discussed in detail in (Fernández-Ruiz et al., 2019a; Zhang and Ohsaki, 2007, 2015).

3. Truncated regular polyhedral tensegrities and the octahedron family as sources of tensegrity structures

3.1 Truncated regular polyhedral tensegrities

It is known that tensegrity structures can be constructed by assembling elementary cells (Li et al., 2010; Pugh, 1976). In the diamond pattern described by Pugh (Pugh, 1976) cables form diamonds or rhombic cells with a strut defining one diagonal (see Figure 1).
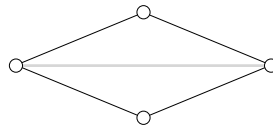

Figure 1. Diamond elementary cell. Black and grey lines represent cables and struts respectively.

Truncated regular polyhedrons are a source of tensegrity structures called "truncated regular polyhedral tensegrities" (Zhang and Ohsaki, 2012; Zhang et al., 2013, 2012). These tensegrities are constructed following the procedure proposed by (Li et al., 2010), according to which the nodes of the truncated regular polyhedral tensegrities coincide with the vertices of the truncated polyhedron. Let us consider the truncated tetrahedron shown in Figure 2.a as an example. The struts connect some vertices of the truncated tetrahedron following the indications proposed in (Li et al., 2010) (see grey lines in

Figure 2.b). Then, rhombic cells are defined (one for each strut) removing and adding some cables as can be seen in Figure 2.c, where only a rhombic cell has been represented for the sake of clarity. It can be clearly seen in Figure 2.c that the cables of the elementary rhombic cells can be classified into two types: type 1 (red lines) and type 2 (blue lines).

In applying the same procedure, rhombic truncated tetrahedral, cubic, octahedral, dodecahedral and icosahedral tensegrities can be obtained (see (Zhang et al., 2013)).

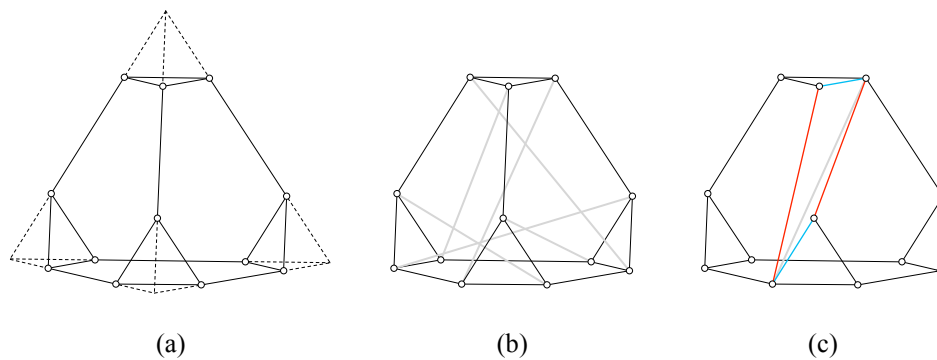(a)   (b)   (c)

Figure 2. (a) Truncated regular tetrahedron, (b) connection of the struts and (c) connectivity pattern of the rhombic truncated tetrahedron. In (c) only a rhombic cell is drawn. Red, blue and grey lines correspond to type 1 cables, type 2 cables and struts, respectively. (For interpretation of the references to color in this figure legend, the reader is referred to the web version of this article).

3.2 The octahedron family

A tensegrity family is a group of tensegrity structures that share a common connectivity pattern (Fernández-Ruiz et al., 2019a). It is considered that a tensegrity belongs to a family if it has as folded forms all the lower members of the family. The octahedron family is composed by three members: the octahedron, the expanded octahedron and the double-expanded octahedron (Fernández-Ruiz et al., 2019a). The first member of the family is the octahedron (see Figure 3.a), which is composed by 15 members (12 cables and 3 struts) and 6 nodes. The expanded octahedron (see Figure 3.b) is the second member of the family, and it has 30 members (24 cables and 6 struts) and 12 nodes. Both tensegrities are well-known tensegrity forms present in numerous works in the

literature. The expanded octahedron is the expansion of the octahedron (as it is indicated by its name), in such a way that each node, cable and strut of the octahedron is duplicated during the expansion process. Based on the expansion from the octahedron to the expanded octahedron, Fernández-Ruiz et al. (Fernández-Ruiz et al., 2019a) obtained the double-expanded octahedron, the third component of the octahedron family (see Figure 3.c). This new tensegrity form is composed by 60 members (48 cables and 12 struts) and 24 nodes. All the components of the octahedron family are formed by the combination of rhombic cells.

It is interesting to remark that in the case of the three members of the octahedron family (Fernández-Ruiz et al., 2019a) represented in Figure 3 only two different q values were considered: q_c for cables and q_b for bars or struts (black and grey lines respectively in Figure 3).
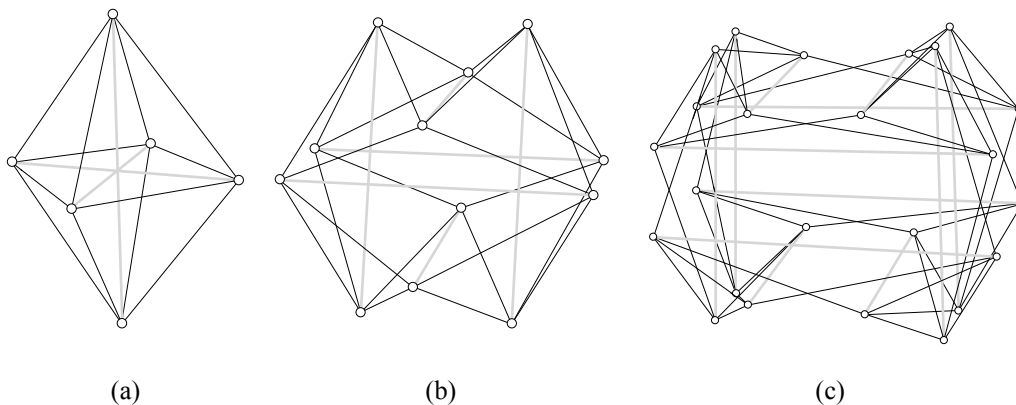

(a) (b) (c)

Figure 3. Octahedron family: (a) octahedron, (b) expanded octahedron and (c) double-expanded octahedron. Black lines correspond to cables and grey lines to struts.

New tensegrity forms can be derived from the octahedron family based on its connectivity pattern, either by the definition of a higher member through an expansion process or by introducing a higher number of different force:length ratio values for cables and struts.

4. Octahedron family. New super-stable tensegrity forms

As commented before, all the cables and struts of the tensegrities of the octahedron family in Figure 3 have the same value of q respectively. Nevertheless, new super-stable tensegrity forms that belongs to the octahedron family can be obtained considering a higher number of q values.

4.1 Octahedron

A plane connection graph is a graphical representation of the connectivity between the nodes of a tensegrity (Fernández-Ruiz et al., 2019a). Figure 4 shows the plane connection graph of the octahedron which has been defined based on the connectivity rules of the octahedron family defined in (Fernández-Ruiz et al., 2019a). The connectivity matrix $\mathbf{C} \in \Re^{15 \times 6}$ of the octahedron can be constructed using the plane connection graph shown in Figure 4 and according to Eq. (1).
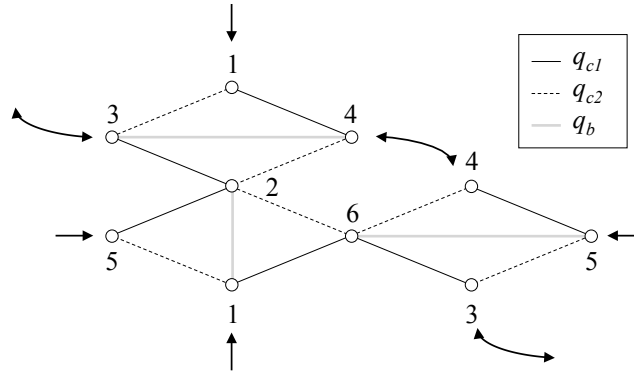

Figure 4. Plane connection graph of the octahedron.

Now three different values of force:length ratio are going to be considered: q_{c1} for type-1 cables (continuous black lines in Figure 4), q_{c2} for type-2 cables (dashed black lines in Figure 4) and q_b for struts (grey lines in Figure 4). Type-1 and type 2 cables have been identified following the pattern of the rhombic elementary cell depicted in Figure 2.c. Then the characteristic polynomial $p(\lambda)$ of the resulting matrix $\mathbf{D} \in \Re^{6 \times 6}$ is computed and the non-degeneracy condition in 3D shown in Eq. (5) is imposed. Two independent normalized force:length ratios taken as $Q_1 = -q_{c1}/q_b > 0$ and $Q_2 = -q_{c2}/q_b > 0$ are considered as in (Zhang et al., 2013). The expressions of the polynomials that conforms

the system of equations $a_1\,(Q_1,\,Q_2) = a_2\,(Q_1,\,Q_2) = a_3\,(Q_1,\,Q_2) = 0$ are shown in

Appendix A (see Eqs .(A1), (A2) and (A3) respectively). As it has been already

explained in Section 2, this system of equations implies that matrix **D** has a rank

deficiency of at least 4. The solutions of the above system of equations are: $\{q_b = 0\}$

(not considered), $\{Q_1 = -1/2;\ Q_2 = 1/2\}$ (not possible because Q_1 is < 0), $\{Q_1 = 1;\ Q_2 = -1\}$ (not possible because Q_2 is < 0) and $\{Q_1 = 1/2;\ Q_2 = 1/2\}$. So, the only possible

solution is $Q_1 = Q_2 = 1/2$, which coincides with the unique solution proposed in

(Fernández-Ruiz et al., 2019a) (that is, $q_{c1} = q_{c2} = -2\ q_b$). This solution leads to the

octahedron (Fernández-Ruiz et al., 2019a) (see Figure 3.a), which is a super-stable

tensegrity form.

4.2 Expanded octahedron

Figure 5 shows the plane connection graph of the expanded octahedron. It can be clearly

seen that the expanded octahedron has twice the number of rhombic cells of the

previous member of the family (the octahedron, see Figure 4). Consequently, the

expanded octahedron has twice the number of nodes, cables and struts in comparison

with the octahedron. The connectivity matrix $\mathbf{C} \in \mathfrak{R}^{30\times12}$ of the expanded octahedron is

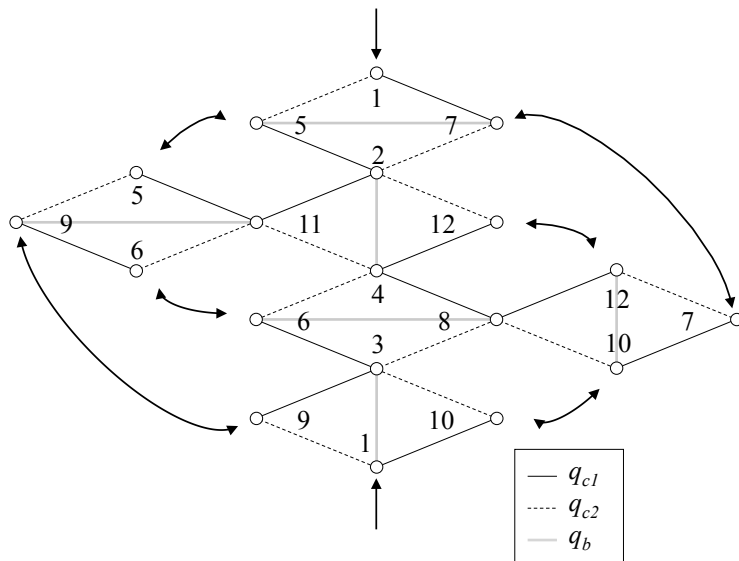defined based on the plane connection graph (see Figure 5).

Figure 5. Plane connection graph of the expanded octahedron

Let us consider again three different values of q: q_{c1} for type-1 cables, q_{c2} for type-2 cables and q_b for struts (continuous black lines, dashed black lines and grey lines in Figure 5 respectively), resulting in $\mathbf{Q} \in \Re^{30 \times 30}$. The characteristic polynomial $p(\lambda)$ of the resulting matrix $\mathbf{D} \in \Re^{12 \times 12}$ is calculated and the system of equations $a_1 (Q_1, Q_2) = a_2 (Q_1, Q_2) = a_3 (Q_1, Q_2) = 0$ solved (the expressions of a_1, a_2 and a_3 can be seen in Eqs. (A4), (A5) and (A6)). The solutions of the system are: $\{q_b = 0\}$ (not considered), $\{Q_1 = 0; Q_2 = 0\}$ (not considered), $\{Q_1 = 1/2; Q_2 = 1/2\}$ and the values shown in Eqs. (7) and (8).

$$Q_2 = \frac{-1 + 4Q_1 - 3Q_1^2 - \sqrt{1 - 2Q_1 + Q_1^2 - 6Q_1^3 + 9Q_1^4}}{3(-1 + 2Q_1)} \tag{7}$$

$$Q_2 = \frac{-1 + 4Q_1 - 3Q_1^2 + \sqrt{1 - 2Q_1 + Q_1^2 - 6Q_1^3 + 9Q_1^4}}{3(-1 + 2Q_1)} \tag{8}$$

The solution $Q_1 = Q_2 = 1/2$ coincides with the solution obtained in the previous subsection. This solution corresponds to the octahedron (see Figure 3.a) but now with two nodes sharing the same position of the space (that is, duplicated nodes). This proves that the octahedron is the folded form of the expanded octahedron (Fernández-Ruiz et al., 2019a).

The self-equilibrated configurations of the expanded octahedron considering three different q values are the ones collected in the previous solutions. However, it has to be pointed out that only some of them satisfy the super-stability conditions defined in Section 2.3. Henceforth, the super-stability of the solutions is studied. Figure 6.a shows the Q_1 - Q_2 curves corresponding to Eqs. (7) and (8). Firstly, the condition $q_b < 0$, $q_{c1} > 0$ and $q_{c2} > 0$ must be fulfilled (which corresponds with $Q_1 > 0$ and $Q_2 > 0$ as stated above). Thus, curve 1 of Eq. (8) and the part of the curve of Eq. (7) which is not in the

region $Q_1 > 0$ and $Q_2 > 0$ must be excluded from the study. Secondly, condition (i) for the super-stability of tensegrity structures requires that the force density matrix **D** must have exactly four zero-eigenvalues. This condition is fulfilled for all the Q_1 - Q_2 pairs of values defined by Eqs. (7) and (8) in the region $Q_1 > 0$ and $Q_2 > 0$ and for the solution $Q_1 = Q_2 = 1/2$. Thirdly, condition (ii) of super-stability requires that matrix **D** should be positive semi-definite. This condition is not fulfilled by the solution $Q_1 = Q_2 = 1/2$ which has some negative eigenvalues, so it is excluded of the super-stability analysis (this has been represented by a small white circle in Figure 6.a). Figure 6.b shows the minimum eigenvalue of matrix **D** obtained from the region $Q_1 > 0$ and $Q_2 > 0$ of the curve corresponding to Eq. (7) (i.e., in the range $0 < Q_1 < 2/3$). It can be seen in Figure 6.b that there is always a negative eigenvalue of **D** in this region and consequently, Eq. (7) is excluded from the study. On the other hand, the matrix **D** corresponding to the values of curve 2 of Eq. (8) is always positive semi-definite. Finally, condition (iii) requires that the geometry matrix **G** (defined in (Zhang and Ohsaki, 2015)) should have a rank of 6 in the case of a three-dimensional tensegrity. The tensegrities defined by curve 2 of Eq. (8) in Figure 6.a have a geometrical matrix **G** with a rank of six. Consequently, all the solutions defined by curve 2 of Eq. (8) fulfill all the super-stability conditions given in Section 2.3 and they are super-stable tensegrity structures. This analysis of the super-stability of the expanded octahedron considering three different q values coincides with the analysis of the stability of rhombic truncated tetrahedral tensegrities carried out in (Zhang et al., 2013). The significant difference is that the same results have been achieved from two different paths: topology in the case of the present paper and geometry in the case of Zhang (Zhang et al., 2013).
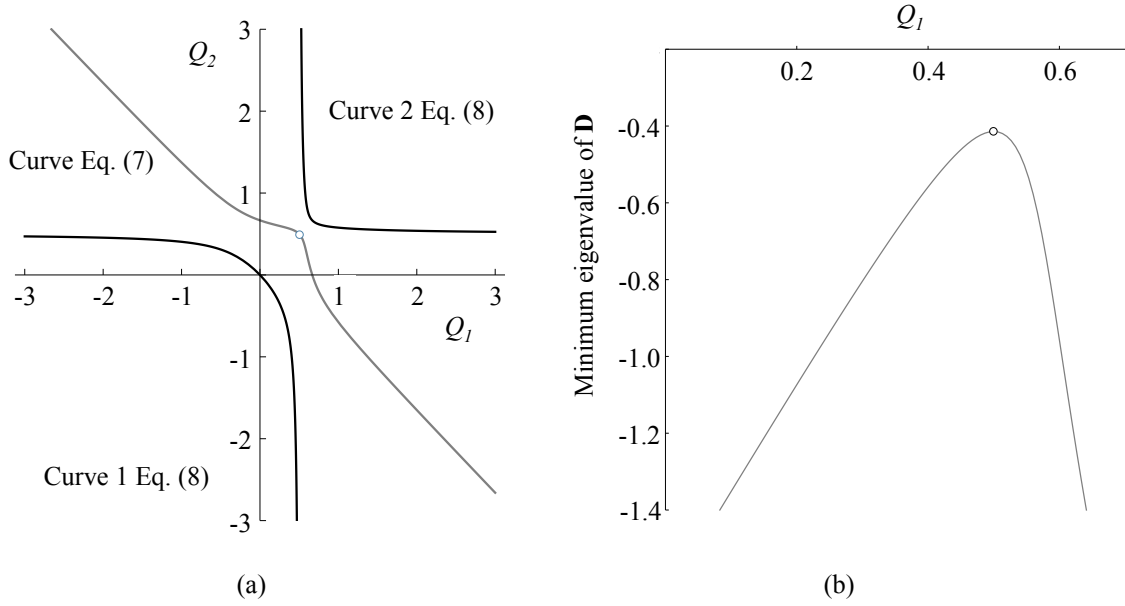
Figure 6. (a) Q_1 - Q_2 **self-equilibrium curves of the expanded octahedron (Eqs. (7) and (8)) and (b) minimum eigenvalue of D for the** Q_1 - Q_2 **curve of Eq. (7) in the region** $Q_1 > 0$ **and** $Q_2 > 0$.

The expanded octahedron has the same q value for all the cables being $q_{c1} = q_{c2} = -2/3$ q_b (Fernández-Ruiz et al., 2019a). If the condition $Q_1 = Q_2$ is introduced in Eq. (8) two solutions are obtained: $Q_1 = Q_2 = 0$ and $Q_1 = Q_2 = 2/3$ (which coincides with $q_{c1} = q_{c2} = -2/3$ q_b, expanded octahedron, see Figure 7.b). The rest of the tensegrity forms defined by curve 2 of Eq. (8) can be considered as part of the octahedron family because all of them share a common connectivity pattern. Thus, the expanded octahedron is a second member of the family together with the solutions corresponding to curve 2 of Eq. (8), see Figure 6.a. Examples of these tensegrity structures are shown in Figure 7. It can be seen that the tensegrities shown in Figure 7.a and 7.c (based on the connectivity pattern of the octahedron family) resembles a truncated tetrahedron. In fact, the well-known expanded octahedron is a rhombic truncated tetrahedral tensegrity with $Q_1 = Q_2$ (Zhang et al., 2013).
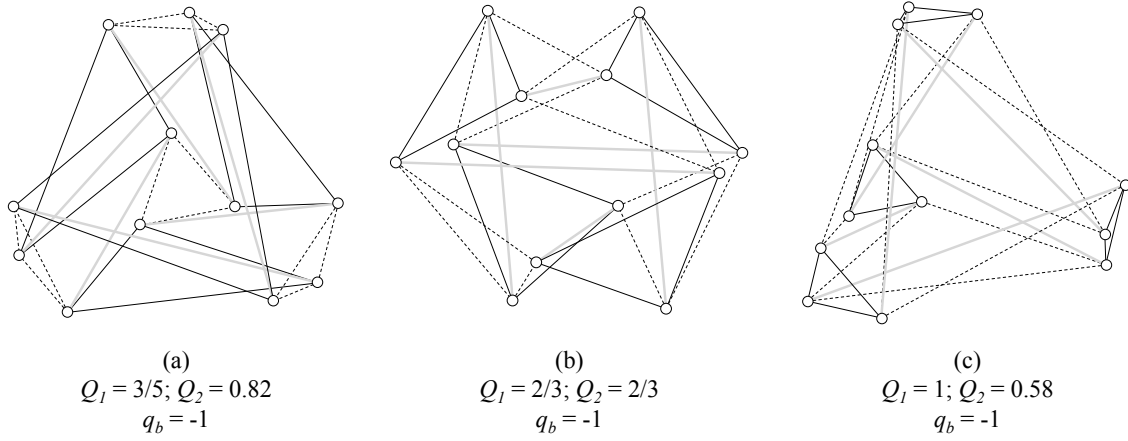
15

<div align="center">

(a)

$Q_1 = 3/5; Q_2 = 0.82$

$q_b = -1$

(b)

$Q_1 = 2/3; Q_2 = 2/3$

$q_b = -1$

(c)

$Q_1 = 1; Q_2 = 0.58$

$q_b = -1$

</div>

Figure 7. Equilibrium shapes obtained from the plane connection graph shown in Figure 5 considering different values of q. (a) $Q_1 = 3/5$ & $Q_2 = 0.82$ (Eq. (8)) & $q_b = -1$, (b) expanded octahedron $Q_1 = 2/3$ & $Q_2 = 2/3$ (Eq. (8)) & $q_b = -1$ and (c) $Q_1 = 1$ & $Q_2 = 0.58$ (Eq. (8)) & $q_b = -1$. Black continuous and dashed lines and grey lines correspond to q_{c1}, q_{c2} and q_b respectively in accordance with Figure 5.

4.3 Double-expanded octahedron

The double-expanded octahedron is a new tensegrity structure introduced in (Fernández-Ruiz et al., 2019a). This tensegrity was defined applying the connectivity pattern of the octahedron family (Fernández-Ruiz et al., 2019a), instead of using geometrical interpretations based on truncated regular polyhedrons as other authors did (Zhang and Ohsaki, 2012; Zhang et al., 2013, 2012). The plane connection graph of the double-expanded octahedron is shown in Figure 8. This tensegrity has twice the number of rhombic cells of the expanded octahedron (see Figure 5) and four times the number of rhombic cells of the octahedron (see Figure 4). The number of nodes, cables and struts follows the same proportionality rule. The connectivity matrix $\mathbf{C} \in \mathfrak{R}^{60 \times 24}$ of the double-expanded octahedron is defined based on the plane connection graph displayed in Figure 8.
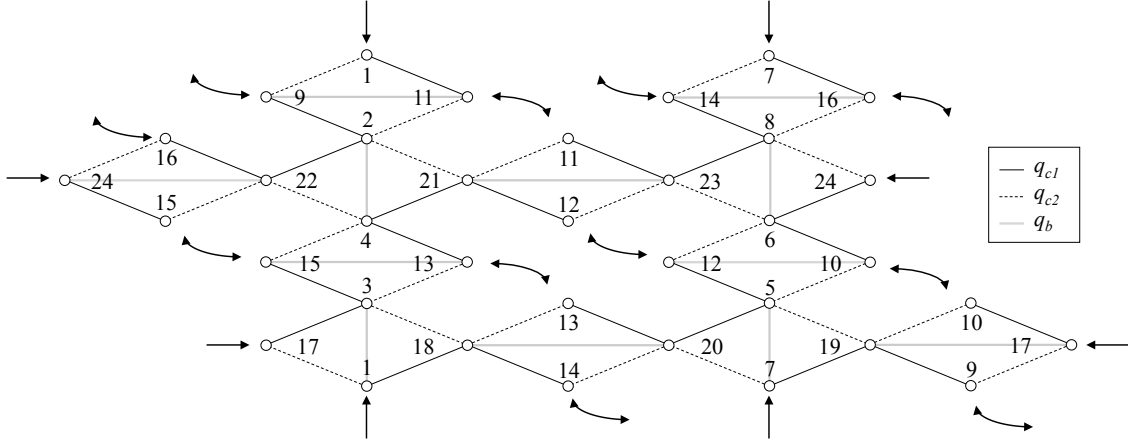
Figure 8. Plane connection graph of the double-expanded octahedron

As in the previous cases, three different values of q are considered: q_{c1} for type-1 cables, q_{c2} for type-2 cables and q_b for struts (continuous black lines, dashed black lines and grey lines in Figure 8 respectively), resulting in $\mathbf{Q} \in \mathfrak{R}^{60 \times 60}$. Once the characteristic polynomial $p(\lambda)$ of $\mathbf{D} \in \mathfrak{R}^{24 \times 24}$ is calculated and the system of equations $a_1 (Q_1, Q_2) = a_2 (Q_1, Q_2) = a_3 (Q_1, Q_2) = 0$ solved (the expressions of a_1 and a_2 can be seen in Eqs. (A7) and (A8), a_3 is not shown due to its length), the following solutions are obtained: $\{q_b = 0\}$ (not considered), $\{Q_1 = -Q_2\}$ (not possible because both Q_1 and Q_2 have to be positive), $\{Q_1 = -1/2; Q_2 = 1/2\}$ (not possible because Q_1 is < 0), $\{Q_1 = 2/3; Q_2 = 0\}$ (not considered because $Q_2 = 0$), $\{Q_1 = 1; Q_2 = -1\}$ (not possible because Q_2 is < 0), $\{Q_1 = 1/3; Q_2 = 1\}$, $\{Q_1 = 1/2; Q_2 = 1/2\}$ and the expressions shown in Eqs. (7), (8), (9) and (10).

$$Q_2 = \frac{1}{4}\left(3 - 6Q_1 - \sqrt{3}\sqrt{3 - 4Q_1 + 12Q_1^2}\right) \tag{9}$$

$$Q_2 = \frac{1}{4}\left(3 - 6Q_1 + \sqrt{3}\sqrt{3 - 4Q_1 + 12Q_1^2}\right) \tag{10}$$

From now on the super-stability condition for each one of the tensegrities corresponding to the obtained solutions is analyzed. The solution $\{Q_1 = 1/2; Q_2 = 1/2\}$ corresponds to the octahedron with all its members and nodes quadruplicated (folded form).

Analogously the solutions given by Eqs. (7) and (8) correspond to the expanded octahedron but in this case with all its members and nodes duplicated (folded form). Because all the self-equilibrium configurations of the previous members of the family are present as folded forms of the double-expanded octahedron, it can be concluded that all of them are members of a same tensegrity family.

Figure 9.a shows the Q_1 - Q_2 curves defined by Eqs. (7), (8), (9) and (10). Firstly, it is necessary to check that Q_1 and $Q_2 > 0$. Based on this condition, curve 1 of Eq. (8), the curve of Eq. (9) and the part of the curves of Eq. (7) and Eq. (10) which are not in the region $Q_1 > 0$ and $Q_2 > 0$ have been excluded from the study. Regarding condition (i) of super-stability, solutions $\{Q_1 = Q_2 = 1/2\}$ and $\{Q_1 = 1/3; Q_2 = 1\}$ have more than 4 zero-eigenvalues and consequently they have also been excluded because of the super-stability requirement. Regarding the condition (ii) of super-stability, matrix **D** should be positive semi-definite. Figure 9.b shows the minimum eigenvalue of **D** corresponding to the Q_1 - Q_2 curves of Eqs. (7), (8) and (10). As in the case of the expanded octahedron, matrix **D** corresponding to the solutions given in Eq. (7) which fulfill $Q_1 > 0$ and $Q_2 > 0$ has negative eigenvalues. Consequently, the equilibrium configurations obtained from Eq. (7) are not considered in this work. The same occurs with the regions $Q_1 > 0.6$ of Eq. (8) and $Q_1 < 0.6$ of Eq. (10) (see Figure 9.b), so all the corresponding equilibrium configurations have been discarded. Consequently, the only regions which lead to positive semi-definiteness of matrix **D** are: $0.5 < Q_1 < 0.6$ of Eq. (8) and $Q_1 > 0.6$ of Eq. (10). It can be verified that both regions fulfill condition (iii) of super-stability. Consequently, tensegrity structures whose force:length ratios satisfy Eq. (8) in the range $0.5 < Q_1 < 0.6$ or Eq. (10) in the range $Q_1 > 0.6$ are super-stable.

It is interesting to note that results shown in Figures 6.b and 9.b have been obtained numerically whereas in the paper a symbolic analysis has been carried out.
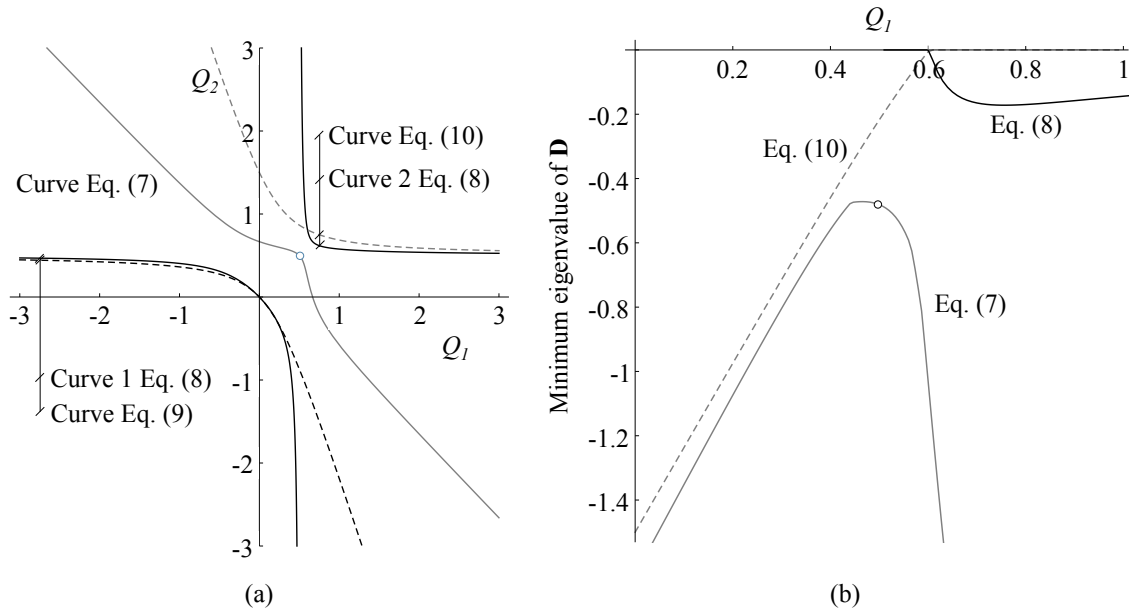
Figure 9. (a) Q_1 - Q_2 **self-equilibrium curves of the double-expanded octahedron (Eqs. (7), (8), (9) and (10)) and (b) minimum eigenvalue of D for the** Q_1-Q_2 **curve of Eqs. (7), (8) and (10) when both** $Q_1 > 0$ **and** $Q_2 > 0$ **are fulfilled.**

Results above show that folded and full forms solutions are collected in different curves. The curve corresponding to Eq. (10) corresponds to full forms whereas Eqs. (7) and (8) and the solution $\{Q_1 = 1/2; Q_2 = 1/2\}$ correspond to folded forms (expanded octahedron and octahedron, respectively). From the previous study, it can be concluded that the only super-stable folded forms of the octahedron family so far are the ones obtained from Eq. (8) in the region $0.5 < Q_1 < 0.6$. On the other hand, the equilibrium configurations obtained from Eq. (10) with $Q_1 > 0.6$ lead to super-stable full forms. The double-expanded octahedron has the same q value for all the cables in such a way that $q_{c1} = q_{c2} = -3/4\ q_b$ (Fernández-Ruiz et al., 2019a). If the condition $Q_1 = Q_2$ is introduced in Eq. (10) two solutions are obtained: $Q_1 = Q_2 = 0$ and $Q_1 = Q_2 = 3/4$ (which coincides with $q_{c1} = q_{c2} = -3/4\ q_b$, i.e. double-expanded octahedron, see Figure 10.a). New super-stable tensegrity forms can be obtained introducing different Q_1 - Q_2 pairs of values according to Eq. (10) with $Q_1 > 0.6$ (see Figure 10.b and 10.c).

(a)
$Q_1 = 3/4; Q_2 = 3/4$
$q_b = -1$

(b)
$Q_1 = 2; Q_2 = 0.59$
$q_b = -1$

(c)
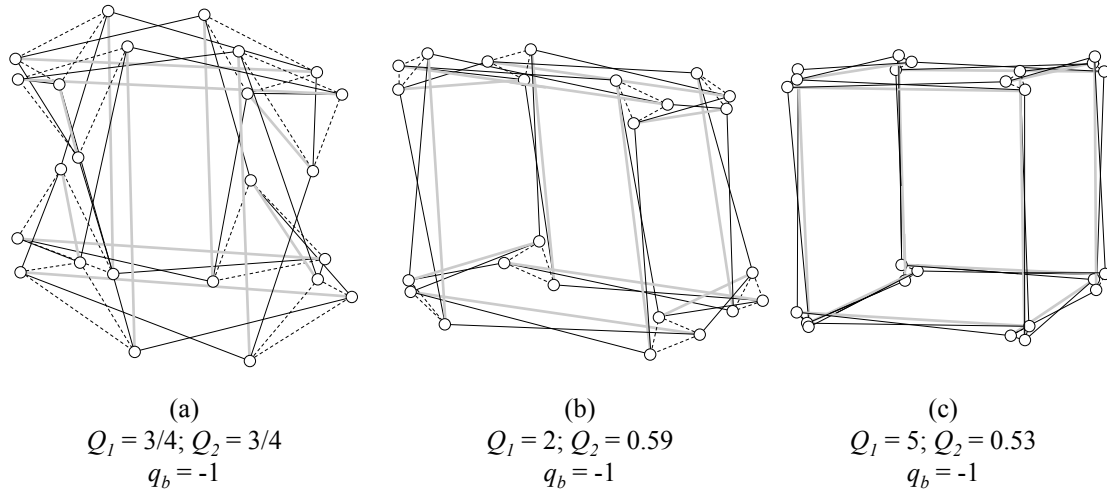$Q_1 = 5; Q_2 = 0.53$
$q_b = -1$

Figure 10. Equilibrium shapes obtained from the plane connection graph shown in Figure 8 considering different values of q. (a) Double-expanded octahedron $Q_1 = 3/4$ & $Q_2 = 3/4$ (Eq. (10)) & $q_b = -1$, (b) $Q_1 = 2$ & $Q_2 = 0.59$ (Eq. (10)) & $q_b = -1$ and (c) $Q_1 = 5$ & $Q_2 = 0.53$ (Eq. (10)) & $q_b = -1$. Black continuous and dashed lines and grey lines correspond to q_{c1}, q_{c2} and q_b respectively in accordance with Figure 8.

It can be clearly seen that, as the value of Q_1 in Eq. (10) increases, the resultant tensegrity resembles more a truncated cube. So, as the expanded octahedron can be geometrically obtained from a truncated tetrahedron (Zhang et al., 2013), the double expanded octahedron can be geometrically obtained from a truncated cube.

In the rhombic truncated cube tensegrity defined in (Zhang et al., 2013), the struts connect some vertices of the truncated cube with the aim of forming rhombic cells as proposed in (Li et al., 2010) (see Figure 11.a). This tensegrity has the same number of nodes, cables and struts than the double-expanded octahedron. However, both tensegrities are not identical because the connectivity between nodes is different. The connectivity pattern of the struts of the double-expanded octahedron can be seen in the truncated cube shown in Figure 11.b. Figure 11.c points out the difference between the connectivity pattern of one of the struts in both tensegrities. Note that the main difference between both tensegrities is that the double-expanded octahedron has been obtained from topology, not by geometrical construction.

Because both types of connection patterns lead to super-stable rhombic tensegrity

structures, it seems evident that more than one rhombic truncated cube tensegrity exists.
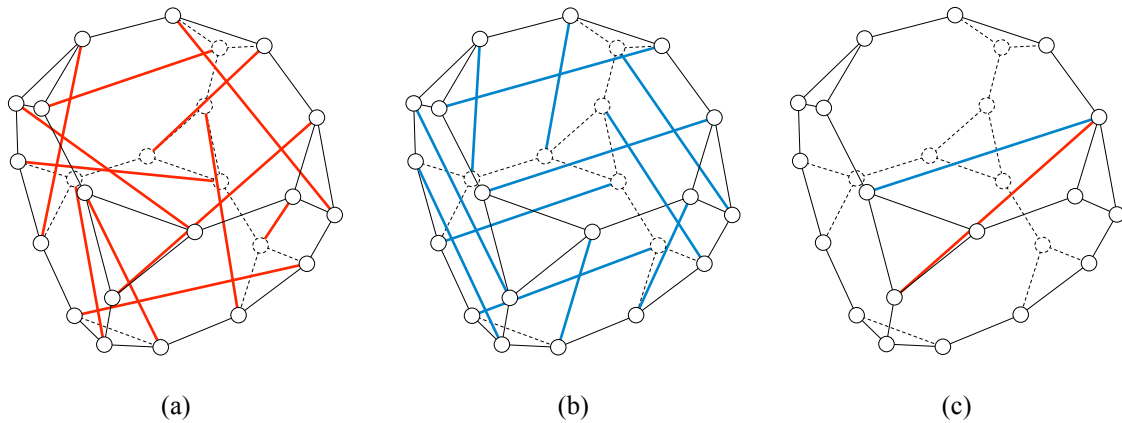

Figure 11. Truncated cube with: (a) strut connectivity of the rhombic truncated cube (Zhang et al., 2013), (b) strut connectivity corresponding to the double-expanded octahedron (Fernández-Ruiz et al., 2019a) and (c) detail of the difference between (a) and (b).

5. Conclusions

The octahedron family has been presented as a new source of tensegrity structures. In the case that only two force:length ratio values are considered (i.e. one for cables and another one for struts) three members of the family are obtained: the octahedron, the expanded octahedron and the double-expanded octahedron. The topology of these tensegrity structures is stablished following a certain connectivity pattern, which is common for the whole family. In this work a higher number of possible q values has been considered. In particular, two types of cables are identified, with different q values. The system of equations resulting from the form-finding problem has been solved analytically and new super-stable tensegrity forms have been obtained. All the tensegrity structures studied in this work belongs to the octahedron family because they have as folded forms all the inferior members of the family.

It has been proved that both the expanded octahedron and the double-expanded octahedron can be obtained geometrically from a truncated tetrahedron and a truncated cube, respectively (as the geometrical constructions proposed in (Zhang et al., 2013)). It

must be highlighted that both relationships truncated tetrahedron – expanded octahedron and truncated cube – double-expanded octahedron has been obtained based on topological patterns, not from geometrical constructions.

Appendix A. Polynomials a_1, a_2 and a_3.

For the octahedron presented in Section 4.1 the polynomials a_1, a_2 and a_3 are the following:

$$a_1 = 18q_b^{5}\left(Q_1 + Q_2\right)^2\left(-2 + 3Q_1 + Q_2\right)^2\left(-1 + 2Q_2\right) \tag{A1}$$

$$a_2 = 3q_b^{4}\left(Q_1 + Q_2\right)\left(-2 + 3Q_1 + Q_2\right)\left(8 - 30Q_1 + 9Q_1^{2} - 38Q_2 + 60Q_1Q_2 + 35Q_2^{2}\right) \tag{A2}$$

$$a_3 = 4q_b^{3}\left(-2 + 3Q_1\left(8 + 9\left(-2 + Q_1\right)Q_1\right) + 24Q_2 + 6Q_1\left(-19 + 18Q_1\right)Q_2 + 3\left(-18 + 35Q_1\right)Q_2^{2} + 28Q_2^{3}\right) \tag{A3}$$

For the expanded octahedron presented in Section 4.2 the polynomials a_1, a_2 and a_3 are the following:

$$a_1 = 576q_b^{11}\left(Q_1 + Q_2\right)^2\left(\left(2 - 3Q_2\right)Q_2 + Q_1^{2}\left(-3 + 6Q_2\right) + Q_1\left(2 - 8Q_2 + 6Q_2^{2}\right)\right)^3 \tag{A4}$$

$$a_2 = 48q_b^{10}\left(Q_1 + Q_2\right)\left(\left(2 - 3Q_2\right)Q_2 + Q_1^{2}\left(-3 + 6Q_2\right) + Q_1\left(2 - 8Q_2 + 6Q_2^{2}\right)\right)^2$$
$$\left(81Q_1^{3} + Q_1\left(-2 + 11Q_2\right)\left(-26 + 33Q_2\right) + 3Q_1^{2}\left(-56 + 121Q_2\right) + Q_2\left(52 + 3Q_2\left(-56 + 27Q_2\right)\right)\right) \tag{A5}$$

$$a_3 = 4q_b^{9}\left(\left(2 - 3Q_2\right)Q_2 + Q_1^{2}\left(-3 + 6Q_2\right) + Q_1\left(2 - 8Q_2 + 6Q_2^{2}\right)\right)$$
$$\left(2187Q_1^{6} + 1458Q_1^{5}\left(-8 + 17Q_2\right) + 9Q_1^{4}\left(1816 + Q_2\left(-8848 + 9469Q_2\right)\right) + \right.$$
$$12Q_1^{3}\left(-640 + Q_2\left(6144 + 7Q_2\left(-2168 + 1491Q_2\right)\right)\right) +$$
$$Q_2^{2}\left(1072 + 3Q_2\left(-2560 + 3Q_2\left(1816 + 81Q_2\left(-16 + 3Q_2\right)\right)\right)\right) +$$
$$2Q_1Q_2\left(1072 + Q_2\left(-11872 + 9Q_2\left(4096 + Q_2\left(-4424 + 1377Q_2\right)\right)\right)\right) +$$
$$\left.Q_1^{2}\left(1072 + Q_2\left(-23744 + Q_2\left(114832 + 3Q_2\left(-60704 + 28407Q_2\right)\right)\right)\right)\right) \tag{A6}$$

For the double-expanded octahedron presented in Section 4.3 the polynomials a_1 and a_2

are the following (a_3 is not shown due to its length):

$$a_1 = 9216 q_b^{23} \left(Q_1 + Q_2\right)^5 \left(-2 + 3Q_1 + Q_2\right)^2 \left(-1 + 2Q_2\right)\left(Q_2\left(-3 + 2Q_2\right) + \right.$$
$$\left. Q_1\left(-3 + 6Q_2\right)\right)^3 \left(\left(2 - 3Q_2\right)Q_2 + Q_1^2\left(-3 + 6Q_2\right) + Q_1\left(2 - 8Q_2 + 6Q_2^2\right)\right)^3 \tag{A7}$$

$$a_2 = 768 q_b^{22} \left(Q_1 + Q_2\right)^4 \left(-2 + 3Q_1 + Q_2\right)\left(Q_2\left(-3 + 2Q_2\right) + Q_1\left(-3 + 6Q_2\right)\right)^2$$
$$\left(\left(2 - 3Q_2\right)Q_2 + Q_1^2\left(-3 + 6Q_2\right) + Q_1\left(2 - 8Q_2 + 6Q_2^2\right)\right)^2$$
$$\left(2349 Q_1^5 \left(1 - 2Q_2\right)^2 + 81 Q_1^4 \left(-1 + 2Q_2\right)\left(70 + Q_2\left(-279 + 250Q_2\right)\right) + \right.$$
$$18 Q_1^3 \left(226 + Q_2\left(-2036 + Q_2\left(6133 + 4Q_2\left(-1860 + 757Q_2\right)\right)\right)\right) + \tag{A8}$$
$$Q_2^2 \left(-888 + Q_2\left(5164 + Q_2\left(-10630 + Q_2\left(9295 + 12Q_2\left(-272 + 27Q_2\right)\right)\right)\right)\right) +$$
$$6 Q_1^2 \left(-148 + Q_2\left(2446 + Q_2\left(-11462 + Q_2\left(22109 + 28Q_2\left(-643 + 173Q_2\right)\right)\right)\right)\right) +$$
$$\left. Q_1 Q_2 \left(-1776 + Q_2\left(15772 + Q_2\left(-48008 + Q_2\left(62729 + 4Q_2\left(-8563 + 1497Q_2\right)\right)\right)\right)\right)\right)$$

References

Bel Hadj Ali, N., Rhode-Barbarigos, L., Smith, I.F.C., 2011. Analysis of clustered tensegrity structures using a modified dynamic relaxation algorithm. Int. J. Solids Struct. 48, 637–647. https://doi.org/10.1016/j.ijsolstr.2010.10.029

Connelly, R., 1998. Tensegrity structures. Why are they stable?, in: Thorpe, M.F., Duxbury, P.M. (Eds.), Rigidity Theory and Applications. Kluwer Academic / Plenum Publishers, pp. 47–54.

Connelly, R., Back, A., 1998. Mathematics and tensegrity. Am. Sci. 86, 142–151. https://doi.org/10.1511/1998.2.142

Estrada, G.G., Bungartz, H.-J., Mohrdieck, C., 2006. Numerical form-finding of tensegrity structures. Int. J. Solids Struct. 43, 6855–6868.

Fernández-Ruiz, M.A., Hernández-Montes, E., Carbonell-Márquez, J.F., Gil-Martín, L.M., 2019a. Octahedron family: The double-expanded octahedron tensegrity. Int. J. Solids Struct. 165, 1–13. https://doi.org/10.1016/j.ijsolstr.2019.01.017

Fernández-Ruiz, M.A., Hernández-Montes, E., Carbonell-Márquez, J.F., Gil-Martín, L.M., 2019b. Form finding of tensegrity structures based on families: the octahedron family, in: 5th International Conference on Mechanical Models in Structural Engineering. Alicante (Spain).

Fernández-Ruiz, M.A., Hernández-Montes, E., Carbonell-Márquez, J.F., Gil-Martín, L.M., 2017. Patterns of force:length ratios for the design of compression structures with inner ribs. Eng. Struct. 148, 878–889. https://doi.org/10.1016/j.engstruct.2017.07.027

Fernández-Ruiz, M.A., Moskaleva, A., Gil-Martín, L.M., Palomares, A., Hernández-Montes, E., 2019c. Design and form- finding of compression structures with prestressing tendons. Eng. Struct. 197, 109394. https://doi.org/10.1016/j.engstruct.2019.109394

Fuller, R.B., 1975. Synergetics - explorations in the geometry of thinking. Macmillan, London, UK.

Graells Rovira, A., Mirats Tur, J.M., 2009. Control and simulation of a tensegrity-based mobile robot. Rob. Auton. Syst. 57, 526–535. https://doi.org/10.1016/j.robot.2008.10.010

Hernández-Montes, E., Fernández-Ruiz, M.A., Gil-Martín, L.M., Merino, L., Jara, P., 2018. Full and folded forms: a compact review of the formulation of tensegrity structures. Math. Mech. Solids 23, 944–949. https://doi.org/10.1177/1081286517697372

Hernández-Montes, E., Jurado-Piña, R., Bayo, E., 2006. Topological Mapping for Tension Structures. J. Struct. Eng. 132, 970–977. https://doi.org/10.1061/(ASCE)0733-9445(2006)132:6(970)

Ingber, D.E., 2003. Tensegrity I. Cell structure and hierarchical systems biology. J. Cell

Sci. 116, 1157–1173. https://doi.org/10.1242/jcs.00359

Ingber, D.E., 1993. Cellular tensegrity: defining new rules of biological design that
govern the cytoskeleton. J. Cell Sci. 104 (Pt 3, 613–27.

Levy, R., Spillers, W.R., 2004. Analysis of geometrically nonlinear structures, 2nd Ed.
ed. Chapman & Hall, London.

Li, Y., Feng, X.Q., Cao, Y.P., Gao, H., 2010. Constructing tensegrity structures from
one-bar elementary cells. Proc. R. Soc. A Math. Phys. Eng. Sci. 466, 45–61.
https://doi.org/10.1098/rspa.2009.0260

Linkwitz, K., Schek, H.J., 1971. Einige Bemerkungen zur Berechnung von
vorgespannten Seilnetzkonstruktionen. Ingenieur-Archiv. 40, 145–158.
https://doi.org/10.1007/BF00532146

Maina, J.N., 2007. Spectacularly robust! Tensegrity principle explains the mechanical
strength of the avian lung. Respir. Physiol. Neurobiol. 155, 1–10.
https://doi.org/https://doi.org/10.1016/j.resp.2006.05.005

Masic, M., Skelton, R.E., Gill, P.E., 2005. Algebraic tensegrity form-finding. Int. J.
Solids Struct. 42, 4833–4858. https://doi.org/10.1016/j.ijsolstr.2005.01.014

Motro, R., 1984. Forms and forces in tensegrity systems, in: Nooshin, H. (Ed.),
Proceedings of Third International Conference on Space Structures. Elsevier,
Amsterdam, pp. 180–185.

Otter, J.R.H., 1965. Computations for prestressed concrete reactor pressure vessels
using dynamic relaxation. Nucl. Struct. Eng. 1, 61–75.
https://doi.org/10.1016/0369-5816(65)90097-9

Pugh, A., 1976. An introduction to tensegrity. University of California Press.

Rhode-Barbarigos, L., Hadj Ali, N.B., Motro, R., Smith, I.F.C., 2010. Designing
tensegrity modules for pedestrian bridges. Eng. Struct. 32, 1158–1167.

https://doi.org/10.1016/j.engstruct.2009.12.042

Schek, H.J., 1974. The force density method for form-finding and computation of general networks. Comput. Methods Appl. Mech. Eng. 3, 115–134. https://doi.org/10.1016/0045-7825(74)90045-0

Tibert, A.G., Pellegrino, S., 2003. Review of Form-Finding Methods for Tensegrity Structures. Int. J. Sp. Struct. 18, 209–223. https://doi.org/10.1260/026635103322987940

Tibert, A.G., Pellegrino, S., 2002. Deployable Tensegrity Reflectors for Small Satellites. J. Spacecr. Rockets 39, 701–709. https://doi.org/10.2514/2.3867

Tran, H.C., Lee, J., 2010. Advanced form-finding of tensegrity structures. Comput. Struct. 88, 237–246. https://doi.org/10.1016/j.compstruc.2009.10.006

Vassart, N., Motro, R., 1999. Multiparameted form-finding method: application to tensegrity systems. Int. J. Sp. Struct. 14, 89–104.

Zhang, J.Y., Ohsaki, M., 2015. Tensegrity Structures. Form, Stability, and Symmetry. Springer.

Zhang, J.Y., Ohsaki, M., 2012. Self-equilibrium and stability of regular truncated tetrahedral tensegrity structures. J. Mech. Phys. Solids 60, 1757–1770. https://doi.org/10.1016/j.jmps.2012.06.001

Zhang, J.Y., Ohsaki, M., 2007. Stability conditions for tensegrity structures. Int. J. Solids Struct. 44, 3875–3886. https://doi.org/10.1016/j.ijsolstr.2006.10.027

Zhang, J.Y., Ohsaki, M., 2006. Adaptive force density method for form-finding problem of tensegrity structures. Int. J. Solids Struct. 43, 5658–5673. https://doi.org/10.1016/j.ijsolstr.2005.10.011

Zhang, L.Y., Li, Y., Cao, Y.P., Feng, X.Q., 2013. A unified solution for self-equilibrium and super-stability of rhombic truncated regular polyhedral

tensegrities. Int. J. Solids Struct. 50, 234–245.

https://doi.org/10.1016/j.ijsolstr.2012.09.024

Zhang, L.Y., Li, Y., Cao, Y.P., Feng, X.Q., Gao, H., 2012. Self-equilibrium and super-

stability of truncated regular polyhedral tensegrity structures: A unified analytical

solution. Proc. R. Soc. A Math. Phys. Eng. Sci. 468, 3323–3347.

https://doi.org/10.1098/rspa.2012.0260